Measured MIMO Capacity and Diversity Gain With Spatial and Polar Arrays in Ultrawideband Channels

Wasim Q. Malik, *Member, IEEE*, and David J. Edwards

Abstract—This paper experimentally investigates the performance of multiple-input multiple-output (MIMO) systems in indoor ultrawideband (UWB) channels. The improvement in robustness and information rate due to spatial and polar antenna arrays is evaluated. The subchannel correlation, power gains of supported eigenmodes, and branch power ratios are analyzed. The polar arrays are found to experience lower correlation than that of spatial arrays. SNR gains of up to 3 and 5 dB are reported with 1×2 and 1×3 spatial arrays, respectively; the latter is shown to double the coverage range. The mutual information capacity is found to scale almost linearly with the MIMO array size, with very low variance. It is confirmed that the device compactness achieved by the polar array comes with only a small penalty in the achievable capacity and SNR gain compared to the spatial array. The multiple-antenna UWB techniques explored in this paper offer the potential for high-data-rate, robust communications.

Index Terms—Antenna arrays, diversity, multiple-input multiple-output (MIMO), polarization, ultrawideband (UWB).

I. INTRODUCTION

ANTENNA diversity techniques have been used extensively in narrowband systems to mitigate temporal and spatial fading [1], [2]. Antenna diversity at the receiver exploits signals with low fading correlation to reduce the probability of outage and improve system robustness. Besides spatial antenna diversity, polarization diversity is a more recently proposed alternative that allows compact antenna arrays with collocated elements [3]–[7]. Other schemes based on angle diversity and pattern diversity have also been presented in literature [2], [8].

Extensions to classical receive diversity have demonstrated the advantage of multiple-input multiple-output (MIMO) arrays for spatial multiplexing to boost the capacity of random fading channels [2], [8]–[11]. Spatial multiplexing transmission schemes offer dramatic improvements in spectral efficiency, and hold great promise for future, high-data-rate wireless systems. In essence, distinct information streams can be transmitted in parallel, exploiting the multiple effective degrees of freedom (EDOFs) [12] enjoyed by MIMO systems.

The majority of the existing work on MIMO systems has focussed on narrowband systems. Only a limited set of theoretical

studies [10], [13] and practical results [14]–[16] are available for wideband and ultrawideband (UWB) MIMO channels. Several MIMO analyses for UWB channels have predicted considerable error-rate improvement [17]–[21]. Spatially multiplexed systems have also been shown to operate well in UWB channels with a large number of resolved multipath components (MPCs) [22]. Capacity expressions for single-input multiple-output (SIMO) and multiple-input single-output (MISO) configurations in Nakagami-faded UWB channels were derived in [23]. Measurement-based analysis has shown that UWB receiver antenna diversity can reduce the required number of rake fingers [24], [25], while spatial multiplexing receivers can offer both diversity and multiplexing gain [26]. Much of the existing work on UWB MIMO is based on simplified channel models, as no UWB spatial channel models exist at this time. An in-depth understanding of this topic is, thus, lacking in the literature primarily due to the dearth of practical results for generalized UWB MIMO channels. The aim of this paper is to fill this vacuum by characterizing MIMO diversity and spatial multiplexing performance in real UWB channels. Our treatment covers SIMO and MIMO configurations for spatial and polar arrays, and intrinsically includes the propagation characteristics of UWB channels [27].

In contrast with narrowband channels, the UWB channel does not suffer from deep power fades due to the inherent frequency diversity [27]. The motivation for UWB antenna diversity is instead derived from the regulatory control on power emission levels, which, in turn, adversely affect the link robustness, coverage range, and data rate. As a severe penalty in throughput and quality of service is experienced beyond short distances, high-data-rate UWB communications systems are severely range-restricted. The increase in SNR offered by antenna diversity can help extend the range, reduce spatial power variations, and enable the use of high-level modulation for higher data rates. A 5-dB gain can, for instance, partially compensate for the transmission loss of a wall, depending on the construction material, thus improving the system operation in a through-wall propagation scenario [28]. The shallow small-scale fading in the UWB channel [27] can, thus, be largely overcome so that a temporally and spatially uniform signal level is maintained and the link margin can be reduced. In addition, UWB MIMO systems have the potential to deliver extremely high data rates over short distances [29].

Recent work in information theory has studied the interplay between MIMO capacity, bandwidth, channel memory, and SNR [30]. The channel bandwidth W and the number of MPCs L strongly influence MIMO performance. It has been shown that MIMO capacity scaling with $N_{\min} = \min\{N_T, N_R\}$

is conditional upon the quadratic growth of L with $N_{\min}$, where N_T and N_R represent the number of transmit and receive antennas, respectively [31]. Also, the spatial multiplexing gain of the wireless channel is bounded by $\min\{N_T, N_R, L\}$ [13]. Similarly, the diversity gain is bounded by $N_T N_R L$ [1]. These results suggest that MIMO systems are especially promising for channels with large L. Typically, L is very large in UWB channels and grows with the array size, so that MIMO performance can be expected to scale well with large-array configurations. In the light of these theoretical results, this paper is inspired by the promise of UWB and MIMO for high-data-rate, reliable communications, and characterizes their predicted synergy.

II. Experimental Configuration

This section describes the methodology for measuring the MIMO channel data used for the analysis in this paper.

A. Channel Sounding

Frequency-domain channel sounding is performed using a computer-controlled vector network analyzer (VNA) [32] in the federal communications comission (FCC) UWB band ($f_l = 3.1$ GHz to $f_h = 10.6$ GHz). A low-noise amplifier with 30 dB gain is connected between the receiving antenna and the VNA input port. The measurement equipment, including the VNA, cables, connectors, and amplifier are calibrated prior to the measurement to remove frequency-selective attenuation and phase distortion. The complex transmission parameter $S_{21}(f)$ of the scattering matrix is measured and recorded. The channel is sounded at $N_f = 1601$ discrete frequency points over the $W = 7.5$ GHz wideband with $\Delta f \approx 4.7$ MHz resolution. The channel coherence bandwidth is evaluated and found to be $W_c \approx 30$ MHz, validating the frequency sampling of the measured channel transfer functions within bins of width Δf, as $\Delta f \ll W_c$.

B. UWB Antennas

The measurement is performed using discone antennas, whose radiation pattern is omnidirectional in the azimuthal plane, and the emitted electric field is linearly polarized, as described in [33]. The return loss of these antennas is verified to be lower than -10 dB within the frequency band of interest. The antennas are at a height of 1.5–2 m from the ground, depending on the measurement scenarios. It is ensured that the antennas are higher than any surrounding clutter. Our choice of omnidirectional antennas stems from two factors: 1) from an applications perspective, indoor wireless networks generally operate in a broadcast configuration, and 2) from a systems perspective, MIMO systems rely on dense multipath propagation that is facilitated by omnidirectional antennas as opposed to high-gain antennas. The specific design of the omnidirectional antenna is unlikely to alter our main results. Compact practical designs, such as bowtie antennas, can be expected to behave in a similar manner. Note that UWB antenna design is a complex problem due to the requirement for constant characteristics over several octaves [27], [33], [34]. This paper does not discuss the specifics of UWB antenna design, but incorporates antenna dis-
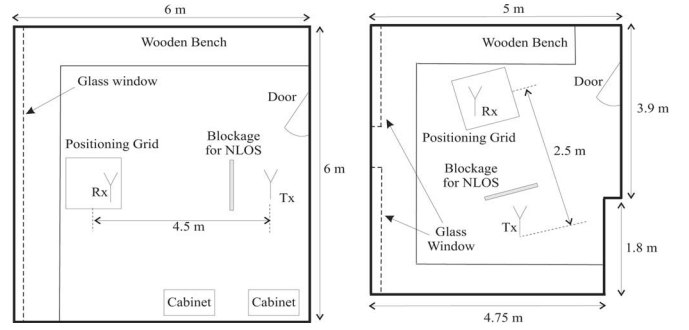

Fig. 1.   Floor layout for the indoor MIMO channel measurements.

tortion effects into the analysis through measurements with real UWB antennas.

C. Measurement Environment

The indoor measurements are conducted within office rooms in two different buildings, as shown in Fig. 1. The walls are made of breeze block, with large glass windows. The rooms contain wooden desks and benches, metallic cabinets, computers, and other scattering objects of various sizes. In each case, line-of-sight (LOS) and non-LOS (NLOS) scenarios are measured. LOS blockage is created by placing a large, thick layer of the RF-absorbent material used in an anechoic chamber, with its cones facing the transmitting antenna. Strict time stationary of the environment is maintained by ensuring complete physical isolation and absence of any mobile objects.

D. Channel Realizations

A computer-controlled receiver positioning grid is used to measure statistically reliable data sets. Thus, each set of measurements is conducted by scanning a $1\,\text{m}^2$ horizontal region. The grid places the receiving antenna at 30 consecutive positions at 0.03 m separation along each dimension of the Cartesian coordinate system. In this manner, 900 individual MIMO channel matrices are obtained. The realizations for various measurement locations are combined into one ensemble with $N_x = 1800$ samples, indexed by $x = \{x_1, \ldots, x_{N_x}\}$. Such data sets are obtained for both LOS and NLOS scenarios.

E. Array Configuration

Two MIMO array types are considered—namely, spatial and polar arrays—with up to three elements at each end. Thus, $N_T \leq 3$ and $N_R \leq 3$, where N_T and N_R represent the transmit and receive array size, respectively. Fig. 2 illustrates the antenna element arrangement for these array configurations.

1) Spatial Array: For the spatial array configuration, we consider the uniform linear array, which is a simple and popular choice for practical spatial diversity systems. The largest wavelength in our analysis is $\lambda_l = c/f_l \approx 0.1$ m, where $c = 3 \times 10^8$ m/s is the speed of light. While the Jakes model may not be directly applicable to the UWB channel, it can nevertheless be used for a coarse approximation of the coherence distance. According to this model, the required interelement separation
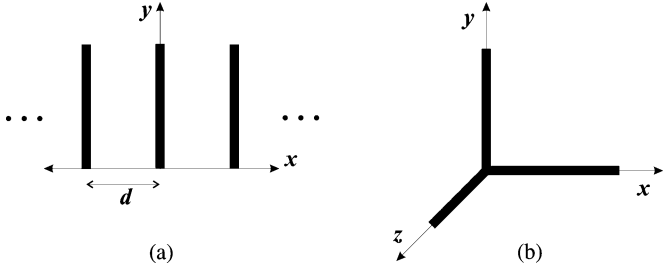
Fig. 2. Two MIMO array configurations. (a) Spatial linear array has interelement spacing d. (b) Tripolar array spans the Cartesian axes.
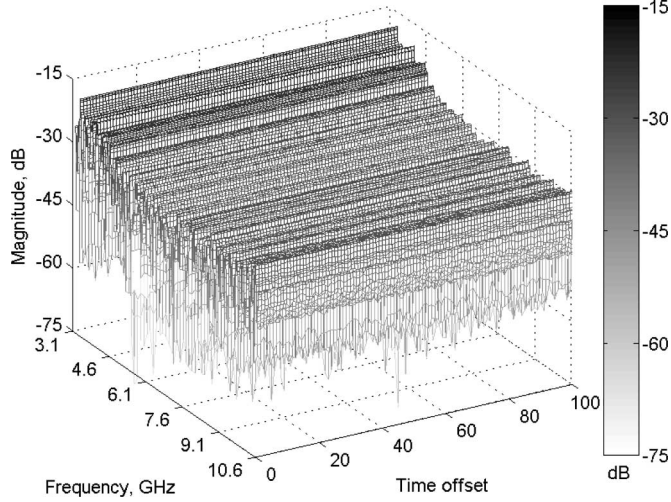

Fig. 3. Indoor UWB channel responses at 10 min time offsets measured using the same transmitter–receiver location in our measurement environment.

for acceptably low fading correlation is $d \geq \lambda/2$ [35]. We, therefore, use $d = 0.06$ m in order to achieve low correlation, which is a requirement for MIMO systems. The arrays are placed in a broadside configuration. We will refer to the individual elements as S_1, S_2, and S_3. The spatial arrays at both transmitter and receiver are synthesized by sequential measurements exploiting the temporal stationarity of the indoor channel. To verify the stationarity, the single-antenna channel response for the vertically polarized, LOS $S_1 \times S_1$ link is measured with 10 min intervals over a 24 h duration. The first 100 channel responses are shown in Fig. 3. From inspection, the measurement environment demonstrates excellent stability and time stationarity, validating the experimental procedure. We have used this approach for virtual array synthesis in our previous work [36]–[38], and similar techniques have also been used in [14], [39], and [40]. Note that the array synthesis approach has a drawback: antenna coupling cannot be directly included in the measurement. Thus, the antenna pattern distortion due to mutual coupling and its potential impact on MIMO capacity [41]–[43] is not considered in this paper.

2) Polar Array: Tripolar MIMO measurements are conducted in a similar manner. Each of the three orthogonally polarized antennas is placed sequentially at the same location, S_1, to synthesize a collocated tripolar array. The use of three orthogonally polarized antennas along the Cartesian axes pro-

vides a basis spanning the entire polarization signal space, and thus, enables the extraction of all three polarized electric field components. In the rest of this paper, the polar antenna elements will be represented by V, H_n, and H_c, corresponding to the vertical and two horizontal orientations of the electric field. The horizontal polarizations H_n and H_c denote the configurations in which the electric field is normal and collinear with the transmitter–receiver line, respectively. The polarization rotation of the omnidirectional, linearly polarized antenna used here inevitably alters its radiation pattern. Therefore, for such an antenna, polarization diversity cannot be decoupled from pattern diversity.

III. SYSTEM MODEL

We represent the xth UWB MIMO channel realization by the three-dimensional matrix $\mathbf{H}^{(x)} \in \mathcal{C}^{N_R \times N_T \times N_f}$ such that $\mathbf{H}^{(x)} = [\mathbf{H}_f^{(x)}]_{f=1}^{N_f}$, where $\mathbf{H}_f^{(x)}$ is the flat-fading MIMO channel matrix at frequency component f. We define the UWB single-input single-output (SISO) channel transfer function between the t-th transmitter and rth receiver as the vector $\mathbf{h}_{r,t}^{(x)} = [h_{r,t,f}^{(x)}]_{f=1}^{N_f}$, $r = \{1, \dots, N_R\}$, $t = \{1, \dots, N_T\}$, where $h_{r,t,f}^{(x)}$ is the measured complex coefficient describing each constituent narrowband SISO channel. Thus, we can write

$$\mathbf{H}^{(x)} = \begin{bmatrix} \mathbf{h}_{1,1}^{(x)} & \cdots & \mathbf{h}_{1,N_T}^{(x)} \\ \vdots & \ddots & \vdots \\ \mathbf{h}_{N_R,1}^{(x)} & \cdots & \mathbf{h}_{N_R,N_T}^{(x)} \end{bmatrix}. \quad (1)$$

We now define $\mathbf{R}_f^{(x)}$ with dimensions $N_{\min} \times N_{\min}$ such that

$$\mathbf{R}_f^{(x)} = \begin{cases} \mathbf{H}_f^{(x)\dagger}\mathbf{H}_f^{(x)}, & \text{if } N_R > N_T \\ \mathbf{H}_f^{(x)}\mathbf{H}_f^{(x)\dagger}, & \text{otherwise} \end{cases} \quad (2)$$

where $(\cdot)^\dagger$ denotes Hermitian transpose, and we correspondingly define $\mathbf{R}^{(x)} = [\mathbf{R}]_{f=1}^{N_f}$. The MIMO channel power is

$$P = \sum_{f=1}^{N_f} \|\mathbf{H}_f^{(x)}\|_F^2 = \sum_{f=1}^{N_f} \text{Tr}\{\mathbf{R}_f^{(x)}\} = \sum_{f=1}^{N_f} \sum_{n=1}^{N_{\min}} \lambda_{n,f}^{(x)} \quad (3)$$

where $\|\cdot\|_F$ denotes the matrix Frobenius norm, $\text{Tr}\{\cdot\}$ denotes the matrix trace, and the $\lambda_{n,f}$ are the eigenvalues of $\mathbf{R}_f$. The $\mathbf{h}_{1,1}^{(x)}$ channel ($S_1 \times S_1$ or $V \times V$) is taken as reference so that

$$\mathbf{H}^{(x)} := \mathbf{H}^{(x)} \sqrt{N_f} \left| \mathbf{h}_{1,1}^{(x)} \right|^{-1} \quad (4)$$

where $|\cdot|$ denotes the l^2-norm. As a result, the power of the reference SISO subchannel, averaged across the frequencies, is normalized to 1. The power-normalization in (4) is different from that used for MIMO systems with equal branch power [14], and is required here to take into account the unequal powers across the polar array [2]. Note that the normalization approach in [2, Sec. 3.4.3] assumes that $|\mathbf{h}_{i,i}^{(x)}|^2 = 1$ and $|\mathbf{h}_{i,j}^{(x)}|^2 = \alpha$, $i \neq j$, $0 \leq \alpha \leq 1$. This condition does not always hold, especially for the $\pm 90°$ dual-polar arrays or tripolar arrays considered in this paper, as the $H_c \times H_n$ subchannel

TABLE I
MEAN COMPLEX CORRELATION COEFFICIENT AMPLITUDES FOR VARIOUS MIMO SUBCHANNELS (⋆ DENOTES THE CORRELATION OPERATOR)

Type	Configuration	Transmit Correlation		Configuration	Receive Correlation		Configuration	Cross-Correlation	
		LOS	NLOS		LOS	NLOS		LOS	NLOS
Spatial	$S_1 S_1 \star S_1 S_2$	0.49	0.34	$S_1 S_1 \star S_2 S_1$	0.46	0.27	$S_1 S_1 \star S_2 S_2$	0.48	0.33
Spatial	$S_1 S_1 \star S_1 S_3$	0.46	0.33	$S_1 S_1 \star S_3 S_1$	0.40	0.28	$S_1 S_1 \star S_3 S_3$	0.44	0.27
Polar	$VV \star VH_n$	0.07	0.08	$VV \star H_n V$	0.08	0.10	$VV \star H_n H_n$	0.20	0.11
Polar	$VV \star VH_c$	0.16	0.18	$VV \star H_c V$	0.23	0.26	$VV \star H_c H_c$	0.12	0.13

experiences comparatively lower coupling in a realistic multi-path environment. In contrast, our MIMO matrix normalization approach is more general and is based on the actual relative branch powers obtained from measurement.

The previous representation is different from that used for narrowband MIMO channels, in which the MIMO channel coefficients are scalar quantities without frequency dependence. A frequency-domain decomposition approach is used in this paper. Under this formalism, the UWB MIMO channel reduces to a set of flat-fading channels, and the existing theory of flat-fading MIMO channels can then be readily extended to the frequency-selective case [2]. Furthermore, this methodology directly relates to VNA-assisted measurement approaches that provide frequency-domain UWB channel data. The results are, however, independent of this choice of analytical technique.

IV. SPATIAL DEGREES OF FREEDOM

The EDOFs of a deterministic channel matrix can be evaluated from its rank. Random matrices arising from fading, however, in general have full rank, and the rank is then not a reliable measure of the EDOF. The subchannel correlation, eigenvalue distributions, and branch power ratios (BPRs) can be used instead to estimate the actual number of independent channels that can be supported by a MIMO system, and also their relative gains.

A. Subchannel Fading Correlation

Uncorrelated fading is a well-established criterion for MIMO performance evaluation [44], [45]. A spatial correlation coefficient of up to 0.5 causes little loss in MIMO capacity or diversity order [46], [47], which is, therefore, commonly accepted as the correlation threshold. On the other hand, a highly correlated channel matrix degenerates into a unit-rank matrix, implying a single EDOF. The MIMO system then provides only the array gain and no spatial multiplexing gain, so that the capacity is upper-bounded by

$$C \leq \log_2(1 + \rho N_R). \qquad (5)$$

Note that diversity order improvement is generally not the key objective of MIMO techniques in UWB channels. Therefore, spatial correlation does not significantly affect the diversity performance as defined in this paper. However, it does play an important role in determining the MIMO capacity.

The complex correlation coefficient of random variables $m \in \mathbf{m}$ and $n \in \mathbf{n}$ is defined as [45]

$$r_{m,n} = \frac{\mathcal{E}\{mn^*\} - \mathcal{E}\{m\}\mathcal{E}\{n^*\}}{\sqrt{(\mathcal{E}\{|m|^2\} - |\mathcal{E}\{m\}|^2)(\mathcal{E}\{|n|^2\} - |\mathcal{E}\{n\}|^2)}}$$

where $\mathcal{E}\{\cdot\}$ denotes expectation and * denotes complex conjugation. In our UWB channel analysis, $\mathbf{m}$ and $\mathbf{n}$ represent the single-antenna frequency-domain channel vectors, so that $\mathbf{m} = \mathbf{h}_{r_i, t_j}^{(x)}$ and $\mathbf{n} = \mathbf{h}_{r_u, t_v}^{(x)}$ can be substituted in the previous expression. We calculate the correlation coefficients in this manner for each transmitter–receiver pair in our measurement.

The transmit correlation is defined as the correlation between the signals transmitted by two antennas and received by a single antenna, while the converse is termed the receive correlation. We also consider the cross-channel correlation in our analysis. As an example, the receive correlation between S_1 and S_2, when the transmitter is S_1, can be found using $\mathbf{m} = \mathbf{h}_{S_1, S_1}^{(x)}$ and $\mathbf{n} = \mathbf{h}_{S_2, S_1}^{(x)}$. As m and n are random quantities, $r_{m,n}$ is also random. In this paper, we characterize $r_{m,n}$ in terms of its magnitude averaged across the ensemble.

Table I shows the measured correlation coefficient statistics for some representative cases. For spatial arrays, both transmit and receive correlation coefficients are lower than 0.5 in LOS, on average, while much lower values are observed in NLOS. Adjacent elements exhibit higher correlation than do distant elements due to the well-known approximately inverse relationship of correlation with interelement spacing. For polar arrays, higher correlation is observed between the V and H_c antennas than between V and H_n. The polar transmit and receive correlation values also increase slightly in NLOS, compared to LOS. Overall, the results imply that cross-polar coupling is negligible, and the polar array correlation is much lower than that obtained for spatial arrays with $d = 0.06$ m.

From this analysis, the subchannel correlation of appropriately designed UWB MIMO systems is within the acceptable threshold, and multiple-antenna UWB systems can, therefore, be expected to provide significant performance gains.

B. Power Gain Analysis

The eigenspectrum of $\mathbf{R}_f^{(x)}$ provides information about the relative strengths of the independent transmission modes supported by the MIMO system [48]. The number of significant or nonvanishing eigenvalues determines the EDOF. Very high
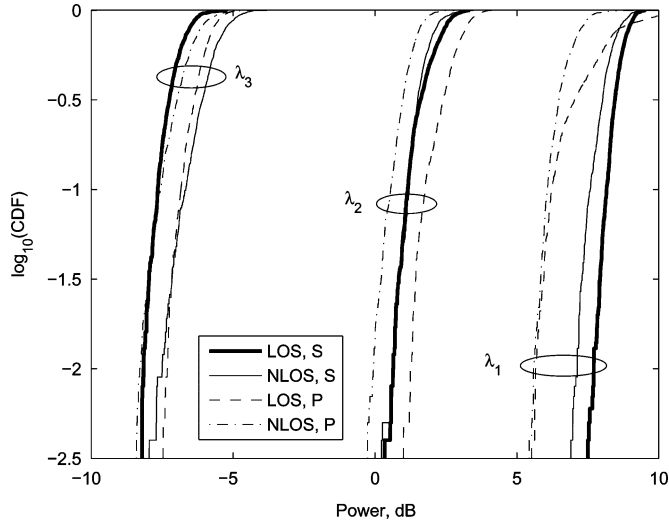
Fig. 4. CDFs of the 3×3 MIMO channel matrix eigenvalues, $\lambda_i, i = 1, 2, 3$, for spatial (S) and polar (P) arrays.

TABLE II
BPR STATISTICS, IN DECIBELS, FOR 1×3 SIMO

Type	Configuration	LOS		NLOS	
		Median	Std. Dev.	Median	Std. Dev.
Spatial	$S_1 \times S_1$	-4.8	0.3	-4.8	0.3
Spatial	$S_1 \times S_2$	-4.8	0.3	-4.8	0.3
Spatial	$S_1 \times S_3$	-4.8	0.3	-4.8	0.3
Polar	$V \times V$	-2.4	0.3	-3.0	0.5
Polar	$V \times H_n$	-4.7	0.5	-3.9	0.5
Polar	$V \times H_c$	-10.9	0.8	-10.2	1.2

correlation between the MIMO subchannels will reduce the number of significant eigenvalues. Under perfect correlation, only one of the eigenvalues is nonzero, while with perfect independence, $N_{\min}$ nonzero eigenvalues are obtained. In the latter case, each subchannel has nonvanishing power gain, and thus, multiple transmission paths can be exploited by a MIMO system [2], [48]. Furthermore, if all the eigenvalues are identically equal to $P/N_{\min}$, a uniform power allocation strategy optimizes the MIMO capacity [2].

Each $\mathbf{R}_f^{(x)}$ can be decomposed into its $N_{\min}$ eigenvalues as $\mathbf{R}_f^{(x)} = \mathbf{Q}_f^{(x)} \mathbf{D}_f^{(x)} \mathbf{Q}_f^{(x)\dagger}$, where $\mathbf{Q}_f^{(x)}$ is an $N_R \times N_T$ unitary matrix and $\mathbf{D}_f^{(x)} = \text{diag}\{\lambda_{n,f}^{(x)}\}$ is a diagonal matrix containing the n eigenvalues of $\mathbf{R}_f^{(x)}$. As $\mathbf{H}_f^{(x)}$ is a random matrix, $\lambda_{n,f}^{(x)}$ are random variates. An analysis of the statistical properties of the eigen spectrum can provide an insight into the corresponding $\mathbf{H}_f^{(x)}$ and its MIMO performance attributes.

For our measured 3×3 MIMO matrices, we compute the eigenvalues, $\lambda_{n,f}^{(x)}$, $n = \{1, 2, 3\}$, and sort them by magnitude to obtain $\lambda_{(n),f}^{(x)}$ such that $\lambda_{(1),f}^{(x)} \geq \lambda_{(2),f}^{(x)} \geq \lambda_{(3),f}^{(x)}$. We then average over frequency to obtain $\lambda_{(n)}^{(x)} = \mathcal{E}_f\{\lambda_{(n),f}^{(x)}\}$. From this ensemble of $N_{\min} = 3$ eigenvalues at each x, we estimate the first-order eigenvalue statistics. Fig. 4 shows the eigenvalue distributions for the three-branch spatial and polar MIMO channels. In each case, three significant eigenvalues are observed, indicating that the power gains of the three subchannels are sufficient for MIMO spatial multiplexing [48]. Also, the largest eigenvalue, $\lambda_{(1)}$, of the polar array is generally smaller than that of the spatial array. The three eigenvalues are also clearly distinct, suggesting power imbalance across the branches. Thus, an optimal power allocation scheme, such as water-filling with transmitter-side channel state information (CSI-T) [2], [49], would be able to achieve better spatial multiplexing performance than that of the uniform power allocation. The analysis in this paper, however,

is limited to MIMO performance under receiver-side channel state information (CSI-R) only.

C. Branch Power Ratios

The performance of a $1 \times N_R$ SIMO diversity system is optimal when the signals incident at the receive antennas have uniform power [6]. The BPR provides a comparison of the signal power levels at the diversity branches (i.e., antennas) [36]. Uniform BPR is especially important for the equal gain combining scheme, where the excess noise contribution from a low signal power branch would otherwise incur an SNR penalty on the combined signal. The BPR of the nth branch at the diversity receiver can be calculated as

$$\text{BPR}_n = 10 \log_{10} \frac{P_n}{P} \qquad (6)$$

where $P_n = \|\mathbf{h}_{n,1}^{(x)}\|_\text{F}^2$ is the wideband power received at the nth branch and P is the total wideband power received by the N_R-element array as defined in (3). It follows that the ideal BPR for each branch in dual- and tri-antenna receive diversity systems is -3 and -4.8 dB, respectively. The BPR is also closely related to cross-polar discrimination (XP), sometimes used to study the performance of polar array systems [7].

Table II shows the estimated first-order statistics of the BPR for each of the spatial and polar antennas when they are taken in 1×3 combinations. The transmitter in each case is the first vertically polarized element, i.e., S_1 or V. The spatial array branches receive identical power levels, with a median value of -4.8 dB. There is, however, a significant power difference in the polar arrays, especially in the LOS environment. The BPR at H_c is the lowest, indicating that the power coupled to that polarization is quite low when a vertically polarized signal is transmitted. This link also experiences greater power variance, as observed from Table II. The reason is that the energy propagated across the $V \times H_c$ link is entirely due to scattering, and does not have the dominant component associated with direct LOS propagation. That is why the BPR of H_c is higher in NLOS than that in LOS. Furthermore, the $V \times V$ link is highly dominant, especially in the LOS environment.

This information predicts that three-branch spatial diversity will perform well in all channel conditions and provide nearly logarithmic SNR gain (in decibel scale), but the performance of a dual-polar diversity system will be sensitive to the antenna orientation and propagation conditions. However, if the application involves stationary antennas, a dual-polar array consisting of the V and H_n elements may be sufficient in terms of the diversity output for certain environments.

V. MIMO PERFORMANCE

This section quantifies the MIMO performance, assuming CSI-R only.

A. Antenna Diversity and SNR Gain

With appropriate combining, an increase in the number of diversity antennas can improve the received signal quality and reduce error rates. Antenna diversity is classically implemented at the receiver, i.e., in SIMO configurations. We now evaluate the $1 \times N_R$ SIMO performance gain with spatial and polar arrays under a maximal ratio combining (MRC) receiver. The transmitter is assumed to be vertically polarized and located at position S_1. In this paper, we define the SNR gain as the difference between the input and output SNRs of the diversity system, which includes the contribution from both diversity gain and array gain. It is well known that antenna diversity performs best under dense multipath propagation, uncorrelated subchannel signals, and equal BPRs. For the indoor UWB channel, these conditions have been analyzed in the preceding discussion. Now, the output SNR of the SIMO antenna diversity system with MRC reception is given by

$$\gamma_{N_R} = \sum_{n=1}^{N_R} \gamma_{(n)} \qquad (7)$$

where $\gamma_{(n)} = P_n/N_0$ is the SNR at the nth branch. Since $\gamma_{(n)} \geq 0 \ \forall \ n$, we have $\gamma_{N_R} \geq \gamma_{(n)} \ \forall \ n$. In the ideal case, the average γ_{N_R} grows by a factor of N_R as the array size is increased, in accordance with aperture theory.

We calculate γ_{N_R} and obtain the SNR gain from it as $\Delta\Gamma = \gamma_{N_R}/\gamma_{(1)}$, where $\gamma_{(1)}$ is the SNR of the $S_1 \times S_1$ or $V \times V$ link for the spatial or polar arrays, respectively. The SNR gain is then converted to decibel scale, and the cumulative distribution function (cdf) of the resulting $\Delta\Gamma_{\mathrm{dB}} = 10 \log_{10}\{\Delta\Gamma\}$ is estimated. These cdfs for the LOS case are shown in Fig. 5. Approximately 3 dB gain is achieved with dual-branch spatial SIMO over SISO, while the addition of another antenna provides another 1.8 dB gain, in accordance with earlier predictions. The case of polarization diversity, however, is markedly different. The polar SIMO system provides a significantly lower gain than does spatial SIMO. This observation confirms the predictions made in Section IV-C. The polar array's diversity performance is also more sensitive to the LOS conditions than that of the spatial array. The reason for the latter's insensitivity to LOS is that the incident multipath power is well distributed among the channel taps, and the LOS path is not dominant in terms of power percentage. Signal depolarization, however, results from scattering,
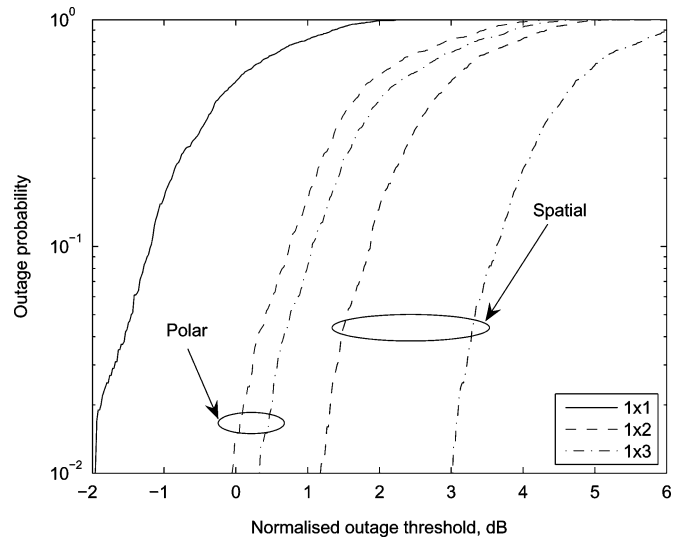

Fig. 5.   SNR gain of $1 \times N_R$ SIMO arrays in spatial and polar configurations, with MRC, under LOS propagation.

and is therefore, inherently dependent on NLOS conditions. We define the $q\%$ outage SNR gain as the improvement in SNR that is guaranteed for $(100 - q)\%$ of the channel realizations; in other words, the probability of an outage event (i.e., the event that the SNR gain for a given realization is less than or equal to the outage SNR gain) is $q\%$ [2]. The 1% outage probability (or 99% reliability) mark is a common and practical figure of merit for diversity performance. Some authors have also used the 10% outage level, but the performance at that mark is very close to that at 1% outage in UWB channels. The median is also sometimes considered, as it indicates the gain achieved in half of the channel realizations. The outage and median SNR gains are listed in Table III, along with the standard deviation. Thus, at 1% outage, the gain is up to 3.1 and 5 dB with two- and three-branch spatial diversity, respectively, while dual- and tripolar diversity boosts the SNR by approximately 1.9 and 2.3 dB, respectively, under LOS. These values are significant compared to up to 5 dB fading typical of the UWB channel [27], showing that antenna diversity systems with small array sizes can be effective in mitigating UWB channel fading. From Table III, the median and 1% outage values of $\Delta\Gamma_{\mathrm{dB}}$ differ by 0.5 dB at most, while its standard deviation is 1 dB or less, due to frequency diversity and the consequently small power variation in UWB channels.

The increase in the receive SNR can be especially beneficial for UWB systems that typically operate at low SNR. This often limits the coverage radius severely, which is currently a major impediment in the widespread deployment of UWB technology. The current implementations of UWB indoor communications systems cannot support very high data rates beyond about 10 m [29]. The SNR improvement achieved by MIMO diversity can be especially useful in extending the coverage range and widening the scope of UWB applications. It can be easily shown that the average coverage range d is related to the pathloss index k through the expression

$$\mathrm{PL}_{\mathrm{dB}} = 10k \log_{10} d \qquad (8)$$

TABLE III
STATISTICS OF THE SNR GAIN, IN DECIBELS, FROM THREE-BRANCH SPATIAL AND POLAR SIMO MEASUREMENTS

Type	Array Size	Configuration	LOS			NLOS		
			1% Outage	Median	Std. Dev.	1% Outage	Median	Std. Dev.
Spatial	1×1	$S_1 \times S_1$	0	0	1.0	0	0	0.8
Spatial	1×2	$S_1 \times S_1 S_2$	3.1	2.9	0.9	3.1	2.9	0.8
Spatial	1×3	$S_1 \times S_1 S_2 S_3$	5.0	4.7	0.9	4.9	4.7	0.8
Polar	1×1	$V \times V$	0	0	0.9	0	0	0.8
Polar	1×2	$V \times V H_n$	1.9	1.8	1.0	2.1	2.6	1.0
Polar	1×3	$V \times V H_n H_c$	2.3	2.2	0.9	2.5	3.0	0.9

where $\mathrm{PL_{dB}}$ denotes the pathloss in decibels, and the constant term representing the pathloss at a reference distance has been omitted. The increase beyond the original range d_0 due to the SNR gain $\Delta\Gamma_{\mathrm{dB}}$ can easily be shown to be

$$\Delta d = d_0 (10^{\Delta\Gamma_{\mathrm{dB}}/10k} - 1). \tag{9}$$

In a UWB indoor LOS environment, $k \approx 1.7$ [50]. In such an environment, a 1×3 SIMO spatial diversity system can extend the range by up to 97% due to its 5 dB gain. If $d_0 = 10$ m, the range achieved with the three-branch SIMO system is 19.7 m. Even larger range improvements can be obtained with MIMO arrays, or with larger array sizes. Thus, antenna diversity can be critical in extending the gamut of UWB applications.

B. Spatial Multiplexing

The MIMO channel capacity quantifies the increase in the information rate achievable with spatial multiplexing, and is a measure of the highest data rate that can be supported over the channel with vanishing error rates. Following the classical Shannon capacity representation, the mutual information, in bits per second per hertz, of a flat-fading MIMO channel without CSI-T is [2]

$$C_f^{(x)} = \log_2 \det \left\{ \mathbf{I}_{N_R} + \frac{\rho}{N_T} \mathbf{R}_f^{(x)} \right\}$$
$$= \sum_{n=1}^{N_{\min}} \log_2 \left\{ 1 + \frac{\rho}{N_T} \lambda_{n,f} \right\}. \tag{10}$$

In (10), $\rho = E_s/N_0$ denotes the average SNR at the receiver antennas, with E_s and N_0 representing the transmitted symbol energy and noise power spectral density, respectively.

An isotropic Gaussian input is reasonable in the absence of CSI-T, and is used in this paper for capacity calculations. The spatial multiplexing gain is quantified in terms of outage capacity and ergodic capacity. The $q\%$ outage capacity is the information rate guaranteed for $(100 - q)\%$ of the channel realizations, while the ergodic capacity is the average information rate over the ensemble of realizations [2].

A special case of MIMO is SIMO, for which (10) becomes

$$C_f^{(x)} = \log_2 \left\{ 1 + \rho \sum_{n=1}^{N_R} \left| h_{n,t,f}^{(x)} \right|^2 \right\}. \tag{11}$$

From (11), SIMO systems can increase the capacity logarithmically with N_R, at best. Under CSI-T, MISO offers similar capacity gain. MIMO systems can, however, establish multiple parallel transmission modes and scale up the capacity by a factor of $N_{\min}$, given uncorrelated subchannels [2].

The capacity of the frequency-selective channel is derived as the expectation of the capacities of its narrowband components. Thus, the wideband capacity expression becomes [2]

$$C^{(x)} = \frac{1}{N_f} \sum_{f=1}^{N_f} C_f^{(x)}. \tag{12}$$

Table IV lists the first-order statistics of capacity estimated from the measured channels assuming CSI-R and 10 dB SNR. The capacities obtained with SISO (1×1), SIMO (1×2 and 1×3), and MIMO (2×2 and 3×3) array configurations are indicated. From the table, the outage capacity achieved with spatial arrays is generally better than that obtained with polar arrays. This is due to the fact that spatial MIMO exhibits approximately equal subchannel power coupling, while in polar MIMO, the $H_c \times H_c$ subchannel, for example, is much weaker than $V \times V$. The gain in SIMO capacity per additional antenna evidently decreases as N_R increases. The MIMO capacity gain, when $N_T = N_R$, however, increases much faster with the array size. With tri-element spatial arrays, the 1% outage capacity can be up to 6.3 b/s/Hz at 10 dB SNR. The capacity does not appear to be strongly dependent on the LOS conditions. This is a significant difference from narrowband channels, which rely on strong scattering and NLOS propagation to produce channels close to the ideal Rayleigh amplitude-distributed channel that can provide a large spatial multiplexing gain. In the infinite bandwidth limit, the mutual information capacity approaches the ergodic capacity under appropriate signaling [31]. Thus, while there is little improvement in the ergodic capacity from the frequency diversity of a frequency-selective channel, the more practical metric, viz., the outage capacity increases significantly. In other words, the

TABLE IV
STATISTICS OF THE MIMO CAPACITY, IN BITS PER SECOND PER HERTZ, AT $\mathrm{SNR} = 10\,\mathrm{db}$, WITH UNIFORM POWER ALLOCATION,
OBTAINED FROM CHANNEL MEASUREMENTS

| Type	Array Size	Configuration	Line-of-sight			Non-line-of-sight		
			1% Outage	Ergodic	Std. Dev.	1% Outage	Ergodic	Std. Dev.
Spatial	1×1	$S_1 \times S_1$	2.3	2.6	0.1	2.5	2.6	0.1
Spatial	1×2	$S_1 \times S_1 S_2$	3.3	3.6	0.1	3.4	3.7	0.1
Spatial	1×3	$S_1 \times S_1 S_2 S_3$	3.9	4.2	0.1	4.0	4.3	0.1
Spatial	2×2	$S_1 S_2 \times S_1 S_2$	4.3	4.7	0.2	4.4	4.8	0.2
Spatial	3×3	$S_1 S_2 S_3 \times S_1 S_2 S_3$	6.2	6.8	0.3	6.3	7.0	0.3
Polar	1×1	$V \times V$	2.3	2.6	0.1	2.4	2.6	0.1
Polar	1×2	$V \times V H_n$	3.0	3.3	0.2	3.1	3.5	0.2
Polar	1×3	$V \times V H_n H_c$	3.1	3.5	0.2	3.3	3.7	0.2
Polar	2×2	$V H_n \times V H_n$	4.3	5.3	0.6	4.4	5.0	0.3
Polar	3×3	$V H_n H_c \times V H_n H_c$	5.6	6.7	0.6	5.5	6.2	0.3
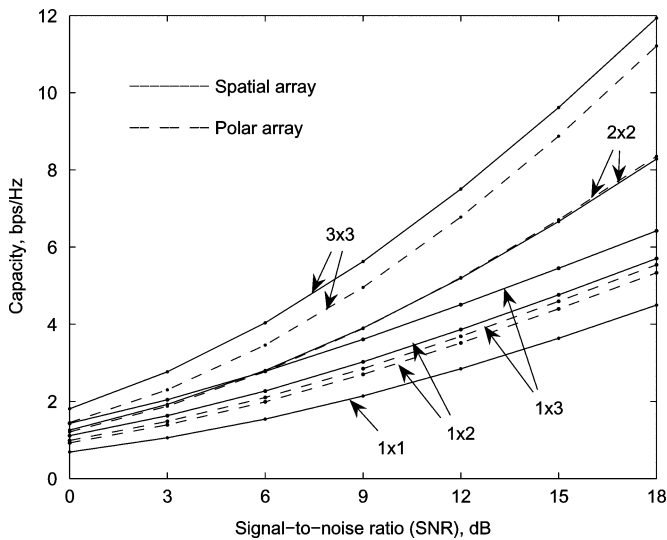
Fig. 6. Capacity of the UWB MIMO channel at 1% outage with spatial and polar arrays under LOS.

capacity of the random wideband channel asymptotically becomes deterministic as the increase in bandwidth tightens the capacity bounds. This was shown experimentally for wideband channels in [14], and our results in Table IV extend this observation to UWB channels. Thus, the experimental value of the 1% outage capacity generally lies within 1 b/s/Hz of the ergodic capacity. These observations confirm that the aforementioned results for wideband channels relating the bandwidth to the variance of capacity can be extended to UWB channels. This result underlines the advantage of MIMO spatial multiplexing with UWB systems and establishes that the combination of the two technologies provides the possibility of future wireless systems with extremely high data rates and reliability.

We next analyze the variation of the outage capacity with the average SNR, and the results are shown in Fig. 6. The large increase in capacity due to MIMO is apparent. Polar MIMO performs almost as well as spatial MIMO irrespective of the SNR. We, thus, note that the polar array provides somewhat lower gain in SNR and capacity than does the spatial array, but offers a feasible alternative for miniaturized UWB devices owing to its compact, collocated antenna structure.

VI. CONCLUSION

MIMO performance has been characterized experimentally in indoor UWB channels for spatial and polar antenna arrays with up to three elements. It has been shown that the MIMO signals are decorrelated sufficiently by the UWB channel at 0.06 m antenna element spacing when the full UWB bandwidth, 7.5 GHz, is used, paving the way for considerable performance gain. Results show that collocated polar arrays experience lower correlation than do spatial arrays. The BPRs are identical for spatial arrays but markedly different for polar arrays, suggesting that the performance of dual-polar systems is highly sensitive to antenna orientation. At 1% outage, two- and three-branch SIMO spatial diversity boosts the SNR by 3 and 5 dB, respectively, and is insensitive to LOS presence, while polar diversity provides a lower SNR gain of up to 2.1 and 2.5 dB. It has been shown that a three-element spatial array at the receiver can double the coverage radius, which can be very useful for wireless personal area network (WPAN) and sensor network applications. With both spatial and polar arrays, the capacity scales almost linearly with the number of antennas at each end in symmetric MIMO configurations. The 1% outage capacity with 3×3 arrays is as high as 6.3 b/s/Hz at 10 dB SNR. The large bandwidth of a UWB system tightens the capacity bounds, and thus, the statistical variation in the SNR and capacity gain is much lower than

that observed in narrowband MIMO channels. This paper has demonstrated that MIMO-enabled UWB systems hold the key to robust, multigigabit links for indoor wireless communication networks.

ACKNOWLEDGMENT

The authors are grateful to A. Kavatjikidis and M. Mtumbuka for assisting with the channel measurements. They also wish to thank B. Allen, C. J. Stevens, A. F. Molisch, and P. J. Smith for insightful discussions.

REFERENCES

[1] S. N. Diggavi, N. Al-Dhahir, A. Stamoulis, and A. R. Calderbank, "Great expectations: The value of spatial diversity in wireless networks," *Proc. IEEE*, vol. 92, no. 2, pp. 219–270, Feb. 2004.

[2] A. J. Paulraj, R. Nabar, and D. Gore, *Introduction to Space–Time Wireless Communications*. Cambridge, U.K.: Cambridge Univ. Press, 2003.

[3] M. R. Andrews, P. P. Mitra, and R. deCarvalho, "Tripling the capacity of wireless communications using electromagnetic polarization," *Nature*, vol. 409, pp. 316–318, Jan. 2001.

[4] S. Kozono, T. Tsuruhara, and M. Sakamoto, "Base station polarization diversity reception for mobile radio," *IEEE Trans. Veh. Technol.*, vol. VT-33, no. 4, pp. 301–306, Nov. 1984.

[5] J.-F. Lemieux, M. S. El-Tanany, and H. M. Hafez, "Experimental evaluation of space/frequency/polarization diversity in the indoor wireless channel," *IEEE Trans. Veh. Technol.*, vol. 40, no. 3, pp. 569–574, Aug. 1991.

[6] A. M. D. Turkmani, A. A. Arowojolu, P. A. Jefford, and C. J. Kellett, "An experimental evaluation of the performance of two-branch space and polarization diversity schemes at 1800 MHz," *IEEE Trans. Veh. Technol.*, vol. 44, no. 2, pp. 318–326, May 1995.

[7] M. Shafi, M. Zhang, A. L. Moustakas, P. J. Smith, A. F. Molisch, F. Tufvesson, and S. H. Simon, "Polarized MIMO channels in 3D: models, measurements and mutual information," *IEEE J. Sel. Areas Commun.*, vol. 24, no. 3, pp. 514–527, Mar. 2006.

[8] C. Oestges and B. Clerckx, *MIMO Wireless Communications*. Orlando, FL: Academic, 2007.

[9] G. J. Foschini and M. J. Gans, "On limits of wireless communications in a fading environment when using multiple antennas," *Wireless Pers. Commun.*, vol. 6, pp. 311–355, Mar. 1998.

[10] I. E. Telatar and D. N. C. Tse, "Capacity and mutual information of wideband multipath fading channels," *IEEE Trans. Inf. Theory*, vol. 46, no. 4, pp. 1384–1400, Jul. 2000.

[11] A. Goldsmith, S. A. Jafar, N. Jindal, and S. Vishwanath, "Capacity limits of MIMO channels," *IEEE J. Sel. Areas Commun.*, vol. 21, no. 5, pp. 684–702, Jun. 2003.

[12] D.-S. Shiu, G. J. Foschini, M. J. Gans, and J. M. Kahn, "Fading correlation and its effect on the capacity of multielement antenna systems," *IEEE Trans. Commun.*, vol. 48, no. 3, pp. 502–513, Mar. 2000.

[13] G. G. Raleigh and J. M. Cioffi, "Spatio-temporal coding for wireless communication," *IEEE Trans. Commun.*, vol. 46, no. 3, pp. 357–366, Mar. 1998.

[14] A. F. Molisch, M. Steinbauer, M. Toeltsch, E. Bonek, and R. S. Thomä, "Capacity of MIMO systems based on measured wireless channels," *IEEE J. Sel. Areas Commun.*, vol. 20, no. 3, pp. 561–569, Apr. 2002.

[15] A. Intarapanich, P. L. Kafle, R. J. Davies, A. B. Sesay, and J. McRory, "Spatial correlation measurements for broadband MIMO wireless channels," in *Proc. IEEE Veh. Technol. Conf. (VTC)*, Los Angeles, CA, Sep. 2004, pp. 52–56.

[16] A. S. Y. Poon and M. Ho, "Indoor multiple-antenna channel characterization from 2 to 8 GHz," in *Proc. IEEE Int. Conf. Comm. (ICC)*, Anchorage, AL, May 2003, pp. 3519–3523.

[17] L.-C. Wang, W.-C. Liu, and K.-J. Shieh, "On the performance of using multiple transmit and receive antennas in pulse-based ultrawideband systems," *IEEE Trans. Wireless Commun.*, vol. 4, no. 6, pp. 2738–2750, Nov. 2005.

[18] L. Yang and G. B. Giannakis, "Analog space–time coding for multiantenna ultra-wideband transmissions," *IEEE Trans. Commun.*, vol. 52, no. 3, pp. 507–517, Mar. 2004.

[19] H. Liu, R. C. Qiu, and Z. Tian, "Error performance of pulse-based ultra-wideband MIMO systems over indoor wireless channels," *IEEE Trans. Wireless Commun.*, vol. 4, no. 6, pp. 2939–2944, Nov. 2005.

[20] M. Weisenhorn and W. Hirt, "Performance of binary antipodal signaling over the indoor UWB MIMO channel," in *Proc. IEEE Int. Conf. Commun. (ICC)*, Anchorage, AL, May 2003, pp. 2872–2878.

[21] W. Siriwongpairat, M. Olfat, and K. J. R. Liu, "On the performance evaluation of TH and DS UWB MIMO systems," in *Proc. IEEE Wireless Commun. Netw. Conf. (WCNC)*, Atlanta, GA, Mar. 2004, pp. 1800–1805.

[22] N. A. Kumar and R. M. Buehrer, "Application of layered space–time processing to ultra wideband communication," in *Proc. Midwest Symp. Circuits Syst.*, Tulsa, OH, Aug. 2002, pp. 597–600.

[23] F. Zheng and T. Kaiser, "On the channel capacity of multiantenna systems with Nakagami fading," in *Proc. EURASIP J. Appl. Signal Proc.*, vol. 2006, pp. 39436-1–39436-11, 2006.

[24] J. Keignart, C. Abou-Rjeily, C. Delaveaud, and N. Daniele, "UWB SIMO channel measurements and simulations," *IEEE Trans. Microw. Theory Tech.*, vol. 54, no. 4, pp. 1812–1819, Apr. 2006.

[25] W. Q. Malik and D. J. Edwards, "UWB impulse radio with triple-polarization SIMO," in *Proc. IEEE Global Commun. Conf. (Globecom)*, Washington, DC, Nov. 2007.

[26] J. Adeane, I. J. Wassell, and W. Q. Malik, "Error performance of ultrawideband MIMO spatial multiplexing systems," presented at the IET UWB Symp., Grenoble, France, May 2007.

[27] B. Allen, M. Döhler, E. E. Okon, W. Q. Malik, A. K. Brown, and D. J. Edwards, *Ultra-Wideband Antennas and Propagation for Communications, Radar and Imaging*. London, U.K.: Wiley, 2006.

[28] T. S. Rappaport, *Wireless Communications: Principles and Practice*. Englewood Cliffs, NJ: Prentice Hall, 2001.

[29] S. Roy, J. R. Foerster, V. S. Somayazulu, and D. G. Leper, "Ultrawideband radio design: The promise of high-speed, short-range wireless connectivity," *Proc. IEEE*, vol. 92, no. 2, pp. 295–311, Feb. 2004.

[30] S. Verdú, "Spectral efficiency in the wideband regime," *IEEE Trans. Inf. Theory*, vol. 48, no. 6, pp. 1319–1343, Jun. 2002.

[31] K. Liu, V. Raghavan, and A. M. Sayeed, "Capacity scaling and spectral efficiency in wide-band correlated MIMO channels," *IEEE Trans. Inf. Theory*, vol. 49, no. 10, pp. 2504–2526, Oct. 2003.

[32] A. M. Street, L. Lukama, and D. J. Edwards, "Use of VNAs for wideband propagation measurements," *Inst. Electr. Eng. Proc. Commun.*, vol. 148, no. 6, pp. 411–415, Dec. 2001.

[33] W. Q. Malik, D. J. Edwards, and C. J. Stevens, "Angular-spectral antenna effects in ultra-wideband communications links," *Inst. Electr. Eng. Proc. Commun.*, vol. 153, no. 1, pp. 99–106, Feb. 2006.

[34] H. G. Schantz, *The Art and Science of Ultra-Wideband Antennas*. Norwood, MA: Artech House, 2005.

[35] W. C. Jakes, *Microwave Mobile Communications*. New York: Wiley, 1974.

[36] L. Lukama, D. J. Edwards, and A. Wain, "Application of three-branch polarization diversity in the indoor environment," *Inst. Electr. Eng. Proc. Commun.*, vol. 150, no. 5, pp. 399–403, Oct. 2003.

[37] M. S. Varela, M. G. Sanchez, L. Lukama, and D. J. Edwards, "Spatial diversity analysis for digital TV systems," *IEEE Trans. Broadcast.*, vol. 47, no. 3, pp. 198–206, Sep. 2001.

[38] M. C. Mtumbuka and D. J. Edwards, "Investigation of a tri-polarized MIMO technique," *Electron. Lett.*, vol. 41, no. 3, pp. 137–138, Feb. 2005.

[39] M. Chamchoy, S. Promwong, P. Tangtisanon, and J.-I. Takada, "Spatial correlation properties of multiantenna UWB systems for in-home scenarios," in *Proc. Int. Symp. Commun. Inf. Technol*, Sapporo, Japan, Oct. 2004, Oct.2004.

[40] C. Prettie, D. Cheung, L. Rusch, and M. Ho, "Spatial correlation of UWB signals in a home environment," in *Proc. IEEE Conf. Ultra-Wideband Syst. Technol. (UWBST)*, Baltimore, MD, May 2002, pp. 65–69.

[41] V. Jungnickel, V. Pohl, and C. von Helmolt, "Capacity of MIMO systems with closely spaced antennas," *IEEE Commun. Lett.*, vol. 7, no. 8, pp. 361–363, Aug. 2003.

[42] M. A. Jensen and J. W. Wallace, "A review of antennas and propagation for MIMO wireless communications," *IEEE Trans. Antennas Propag.*, vol. 52, no. 11, pp. 2810–2824, Nov. 2004.

[43] J. W. Wallace and M. A. Jensen, "Mutual coupling in MIMO wireless systems: A rigorous network theory analysis," *IEEE Trans. Wireless Commun.*, vol. 3, no. 4, pp. 1317–1325, Jul. 2004.

[44] O. Fernandez, M. Domingo, and R. P. Torres, "Empirical analysis of the correlation of MIMO channels in indoor scenarios at 2 GHz," in *Inst. Electr. Eng. Proc. Commun.*, vol. 152, no. 1, pp. 82–88, Feb. 2005.

[45] P. Kyritsi, D. C. Cox, R. A. Valenzuela, and P. W. Wolniansky, "Correlation analysis based on MIMO channel measurements in an indoor environment," *IEEE J. Sel. Areas Commun.*, vol. 21, no. 5, pp. 713–720, Jun. 2003.

[46] M. Chiani, M. Z. Win, and A. Zanella, "On the capacity of spatially correlated MIMO Rayleigh-fading channels," *IEEE Trans. Inf. Theory*, vol. 49, no. 10, pp. 2363–2371, Oct. 2003.

[47] R. O. LaMaire and M. Zorzi, "Effect of correlation in diversity systems with Rayleigh fading, shadowing, and power capture," *IEEE J. Sel. Areas Commun.*, vol. 14, no. 3, pp. 449–460, Apr. 1996.

[48] J. B. Andersen, "Array gain and capacity for known random channels with multiple element arrays at both ends," *IEEE J. Sel. Areas Commun.*, vol. 18, no. 11, pp. 2172–2178, Nov. 2000.

[49] D. Tse and P. Viswanath, *Fundamentals of Wireless Communication*. Cambridge, U.K.: Cambridge Univ. Press, 2005.

[50] S. S. Ghassemzadeh, R. Jana, C. W. Rice, W. Turin, and V. Tarokh, "Measurement and modeling of an ultra-wide bandwidth indoor channel," *IEEE Trans. Commun.*, vol. 52, no. 10, pp. 1786–1796, Oct. 2004.

Wasim Q. Malik (M'00) received the B.E. degree from the National University of Sciences and Technology, Rawalpindi, Pakistan, in 2000, and the D.Phil. degree from the University of Oxford, Oxford, U.K., in 2005, both in electrical engineering.

From 2005 to 2007 he was a Research Fellow at the University of Oxford and a Junior Research Fellow in science at Wolfson College, Oxford. Since 2007, he has been a Postdoctoral Research Fellow at the Massachusetts Institute of Technology, USA. He is an Editor of the book *Ultra-Wideband Antennas and Propagation for Communications, Radar and Imaging* (U.K.: Wiley, 2006) and a Guest Editor of the *Institution of Engineering and Technology (IET) Microwaves Antennas and Propagation* special issue on "Antenna systems and propagation for future wireless communications," 2007. He routinely serves on the organizing and technical program committees of various international conferences. He is the author or coauthor of more than 60 papers published in refereed journals and conferences.

Dr. Malik received the Lindemann Science Fellowship in 2007, the Best Paper Award in the ARMMS RF & Microwave Conference (Steventon, U.K., April 2006) and the Association for Computing Machinery (ACM) Recognition of Service Award in 1997. He is a member of the IEEE.

David J. Edwards received the B.Sc. degree in physics, in 1973, M.Sc. degree in physics of materials, in 1974, and the Ph.D. degree in engineering, in 1987, all from Bristol University, U.K.

He is a Professor of engineering science at the University of Oxford, Oxford, U.K., and a Fellow of Wadham College, Oxford. He has been an academic for 21 years. He was also with the British Telecom. He has a strong record of innovation in communications systems, techniques, and technologies. He is the author or coauthor of more than 300 publications. His current research interests include electromagnetics, magneto-inductive waveguides, ultrawideband communications, *ad hoc* networks, and multiple-input multiple-output (MIMO) systems. He holds many patents and several have appeared as licensed commercial products. He has been a consultant to a large number of industrial organizations.

Prof. Edwards is the recipient of a number of awards and prizes and has been extremely well supported by funding from research councils, industry, and government agencies. He has been a member of a number of national and international committees relating to the antennas and propagation fields. He is a Fellow of the Institution of Engineering and Technology and the Royal Astronomical Society.